https://doi.org/10.5194/amt-2023-103
Preprint. Discussion started: 11 July 2023

Atmospheric Measurement Techniques Discussions

Absolute radiance calibration in the UV and visible spectral range using atmospheric observations during twilight

Thomas Wagner, and Jānis Puķīte

Satellite Remote Sensing Group, Max Planck Institute for Chemistry, Mainz, Germany

Correspondence to: Thomas Wagner (thomas.wagner@mpic.de)

Abstract. We present an improved radiance calibration method based on the calibration method by Wagner et al. (2015). The updated method uses only measurements during the twilight period instead of several hours as for the original method. The calibration is based on the comparison of measurements and simulations of the radiance of zenith-scattered sun light. The main advantage of our method compared to radiance calibration methods in the laboratory is that the calibration can be directly applied in the field. This allows routine radiance calibrations whenever the sky is clear during twilight. The calibration can also be performed retrospectively, and will thus be applicable for the large number of existing data sets. Also, potential changes of the instrument properties during transport from the laboratory to the field are avoided. The new version of the calibration method presented here has two main advantages: First, the required measurement period can be rather short (only a few minutes during twilight for cloud-free conditions). Second, even without knowledge of the aerosol optical depth, the errors of the calibration method are rather small, especially in the UV spectral range where they range from about 4 % at 340 nm to 8 % at 420 nm. If the AOD is known, the uncertainties are even smaller by about a factor of two. For visible wavelengths, good accuracy is only obtained if the AOD is approximately known with uncertainties from about 4 % at 420 nm to 10 % at 700 nm (generally the AOD is nevertheless smaller in the visible than in the UV spectral range). One shortcoming of the method is that it is not possible to determine the AOD exactly at the time of the (twilight) measurements, because AOD observations from sun photometer measurements or the MAX-DOAS measurements are usually not meaningful for such high SZA. But the related uncertainty can be minimised by repeating the radiance calibrations during the twilight periods of several days.

1. Introduction

Measurements of the atmospheric radiance are important for many applications, e.g. atmospheric remote sensing, studies of atmospheric photochemistry, optimisation of the energy yield of photovoltaic cells, or the quantification of biologically relevant UV doses (for more details see e.g. Riechelmann et al., 2013, Wagner et al., 2015). Usually, measurements of the spectral radiance are calibrated in the laboratory using calibrated light sources (e.g. Pissulla et al., 2009; Yu et al., 2014, Niedzwiedz et al., 2021). Uncertainties of the calibration procedures typically range from 3 to 10 % (Wuttke et al., 2006; Pissulla et al., 2009). However, in comparison studies differences between individual instruments up to 30 % have been reported (Pissulla et al., 2009). One particular problem arises from the fact that during transport of the instrument from the laboratory to the field the instrument properties might change.

In this study we build on a recently introduced radiance calibration method using atmospheric radiance measurements in zenith direction (Wagner et al., 2015). In the original study, the radiance calibration was performed by the comparison of measured and simulated zenith radiances under favorable conditions (cloud-free sky, stable aerosol conditions). But in contrast to rather long measurement periods needed with the original method (several hours), the updated method can be applied for much shorter periods (usually a few minutes) during twilight (thus measurements at lower SZAs are not required in the new method). The original and the updated method are based on the comparison of atmospheric radiance

https://doi.org/10.5194/amt-2023-103
Preprint. Discussion started: 11 July 2023

Atmospheric Measurement Techniques Discussions

measurements to atmospheric radiative transfer simulations for a cloud-free atmosphere and low and stable aerosol abundance. One important advantage compared to calibration measurements in the laboratory is that the calibration can be applied directly in the field without the need to transport the instrument to the laboratory and back. Compared to the original method (Wagner et al., 2015), the updated method also requires less specific and less stable atmospheric conditions, especially with respect to the aerosol load. Moreover, during twilight, aerosols have a rather weak effect on the observed radiance (Fig. 1a), especially in the UV. The small influence of atmospheric aerosols on the zenith scattered solar radiance in the UV can be explained by the fact that during twilight the altitude, from which the solar light is scattered into the instrument, increases with decreasing wavelengths because of the increased probability of Rayleigh scattering (Fig. 2). Thus, scattering by aerosols (which usually reside close to the surface) does not substantially increase the observed radiance (as will be shown later, absorbing aerosols might still have a relatively strong effect). Another advantage of the new method is that the pointing accuracy is much less important compared to the original method. In Fig. 1b measured zenith radiances from MAX-DOAS measurements during September and October 2022 are shown. The light blue dots represent all measurement conditions, whereas the dark blue dots represent only clear sky conditions (4.5 days). Like for the simulated radiances, also the measured zenith radiances for clear sky conditions show only small variations, especially during twilight. Between 88° and 90°, the deviation from a fitted polynomial (within the SZA interval 85° to 93°) is about ±1.5 % and ±4 % at 345 nm at 445 nm, respectively (Fig. 1c). During these clear days, the AOD measured by a sun photometer at the same location (https://aeronet.gsfc.nasa.gov/new_web/index.html) varied between 0.08 and 0.18 at 340 nm and between 0.05 and 0.13 at 440 nm.

In this study we explore the applicability of the new method based on radiative transfer simulations, in particular we determine the optimum SZA range. We also quantify the remaining uncertainties caused by incomplete knowledge of the atmospheric state, the position of the instrument, the surface albedo, and possible errors of the measurements and radiative transfer simulations.

The paper is structured as follows: In section 2 the radiative transfer simulations are described and sensitivity studies on the influence of atmospheric aerosols on the zenith scattered sun light during twilight are presented. In section 3 the new method is applied to measurements and the results are compared to the calibration results of the original study. Section 4 provides a summary and conclusions.

2 Radiative transfer simulations

In the first part of this section the radiative transfer model and the atmospheric settings used for the simulations are introduced. In the following parts the effects of aerosols and of other atmospheric and measurement parameters on the simulated zenith scattered radiances are explored. Based on these results the optimum SZA range for the application of the method is determined and the remaining uncertainties are quantified.

2.1 Radiative transfer model and atmospheric scenarios

In the original study, the radiative transfer model MCARTIM-3 (Deutschmann et al., 2011) was used. Because of the rather low radiances during twilight, in this study we decided to use the radiative transfer model SCIATRAN, version 3.8.11 (Rozanov et al., 2017; Mei et al., 2023, https://www.iup.uni-bremen.de/sciatran/) in order to minimise the uncertainties due to noise of the simulations and the computational effort. For the conditions of this paper, the zenith scattered radiances during twilight, simulated by both models agree within ±1%. For the radiative transfer simulations the vertical resolution was 50 m below 2 km, about 1 km between 2 km and 18 km, and up to a few kilometers above.

https://doi.org/10.5194/amt-2023-103
Preprint. Discussion started: 11 July 2023

Atmospheric Measurement Techniques Discussions

Further settings of the simulations are summarised in Table 1. Zenith radiances are simulated for the SZA range from 85° to 93° for the wavelength range 340 nm to 700 nm (in steps of 40 nm).

2.2 Dependence on the AOD

The dependence of the simulated radiance on the AOD for the standard settings (Table 1) is shown in Fig. 3 and Fig. A1 in the appendix. The effect of the AOD increases towards longer wavelengths with deviations of about 7 % and 30 % at 340 nm and 700 nm, respectively (for an SZA of 90° and an AOD of 0.5 compared to an AOD of 0). This is a result of the increase of the penetration depth of the direct sun light into the atmosphere towards longer wavelengths. Thus scattering by aerosols (in addition to Rayleigh scattering) becomes increasingly important towards longer wavelengths. Here it is worth noting that in general the AOD decreases with increasing wavelength. Another important finding is that overall the smallest effects of aerosols are found for SZA around 89° to 90°.

2.3 Uncertainties caused by other atmospheric and surface properties

In Fig. 4 and Fig. A2 the ratios of the simulated radiances compared to those of the corresponding standard scenarios (see Table 1) for two selected AODs (0.1 and 0.3) are shown. These AODs were chosen, because they represent typical conditions in most parts of the world. It is again found that overall the uncertainties increase towards longer wavelengths with deviations of about ± 3 % and ± 6 % at 340 nm and 700 nm, respectively (for an SZA of 90°). For short wavelengths, variations of the temperature and pressure profiles, or the aerosol single scattering albedo have the strongest effect on the simulated radiances. Towards longer wavelengths, the effects of the aerosol phase function and stratospheric aerosols become increasingly important. Overall, again, for SZA around 89° to 90° the smallest deviations are found.

2.4 Uncertainties related to errors of the instrument calibration or the chosen options of the radiative transfer simulations

In this section the effect of the altitude of the instrument, its elevation angle calibration and the chosen options of the radiative transfer model (consideration of polarisation and/or Raman scattering) are investigated. In Fig. 5 and Fig. A3 the ratios of the simulated radiances for these modifications compared to the radiances for the standard settings are shown. Overall, the related uncertainties are rather small (below 2% for most cases). Like before, in general the uncertainties increase towards longer wavelengths, but for an SZA of 90° they are within ± 1 % for all wavelengths.. The rather large deviations due to the neglect of Raman scattering in the radiative transfer simulations for short wavelengths is caused by the increased probability for multiple scattering and is related to the specific location of the chosen wavelength. At 340 nm the sun spectrum has a local maximum, whereas at 380 nm and 420 it has a local minimum (Fraunhofer line).

2.5 Quantification of the uncertainties

This section summarises the different uncertainties investigated in the subsections before. The resulting errors are quantified for the SZA range from 89° to 90°, for which overall the smallest uncertainties were found.

In the first subsection (2.5.1) the errors are quantified for situations when the AOD is known, e.g. from sun photometer observations (Volz, 1959; Tanre et al., 1988; Kaufman et al., 1994; Holben et al., 1998, and references therein) or MAX-DOAS measurements themselves (e.g. Hönninger et al., 2004; Wagner et al., 2004, Friess et al., 2006; Irie et al., 2008; Clémer et al., 2010, and references therein). Again, two scenarios, one with an AOD of 0.1±0.05, and another with an AOD

https://doi.org/10.5194/amt-2023-103
Preprint. Discussion started: 11 July 2023

Atmospheric Measurement Techniques Discussions

of 0.3 ± 0.05 were chosen, which represent typical conditions for most parts of the globe. To account for possible temporal changes of the AOD (MAX-DOAS and AERONET inversions are usually restricted to SZA < 80°), the radiance calibration measurements might be carried out during the twilight period on several succeeding days.

In the second subsection (2.5.2) larger uncertainties for the AOD are assumed (0.25±0.125). This case represents typical aerosol loads for most parts of the globe (except very polluted locations) and might still allow useful radiance calibrations in the UV for situations when the AOD is unknown.

The uncertainties are quantified by variations of the corresponding input parameters as summarised in tables 1 and 2.

2.5.1 Uncertainties if AOD is known

Fig. 6 summarises the individual and total uncertainties for the cases when the AOD is known within ±0.05 (for the specific assumptions see table 2). The sub figures show the error budgets for AODs of 0.1 and 0.3, which represent typical aerosol abundances. The assumptions for the individual error sources (see table 2) are a little bit arbitrary but should represent realistic measurement conditions. Users of the method should check whether these assumptions are realistic for their measurements and could adjust them if needed. The total error is calculated from the individual errors by assuming that all errors are independent. For both scenarios, with the assumptions made in table 2, the dominant error source is the uncertainty of the AOD. However, for the higher AOD of 0.3 also other aerosol-related parameters like the phase function, the SSA or the effect of stratospheric aerosols become important, especially towards longer wavelengths. Overall the uncertainties are still rather small ranging from ±2% for 340nm (AOD = 0.1) to about ±10% for 700nm (AOD = 0.3). Here it should be taken into account that usually the AOD decreases towards longer wavelengths. Thus the total errors for high AOD and long wavelengths probably overestimate the uncertainties for typical scenarios.

2.5.2 Uncertainties if AOD is not known

Fig. 7 summarises the individual and total uncertainties for typical cases when the AOD is not known. For the simulations an AOD of 0.25±0.125 was assumed. Again, the dominant error source is the uncertainty of the AOD, and the uncertainties are much larger than for the two cases with known AOD discussed above. However, for the UV radiances the uncertainties are still rather small, about ±4% at 340nm and ±8% at 420nm.

3 Application to measurements and comparison to results from previous calibration method

The validation of the method using measured data is difficult, because without dedicated campaigns, reference data sets at the same location as the DOAS measurements are usually not available. Thus, like in the original study (Wagner et al., 2015), we apply the method to MAX-DOAS measurements made during the CINDI (I) campaign in Cabauw, The Netherlands, during the morning of 24 June 2009 (Piters et al., 2012). This procedure enables a direct comparison of the calibration results of the original and refined method. The calibration factors are derived from the comparison of the measured radiances (in ‚counts' per second) to the simulated radiances (in $Wm^{-2}nm^{-1}sr^{-1}$).

For the measurements on 24 June 2009 no zenith measurements were conducted exactly at SZAs of 89° and 90°, because of the rather long elevation sequences (in addition to the zenith view, one elevation sequence included also 11 measurements in non-zenith direction). However, zenith measurements were taken close to those SZAs, i.e. at SZAs of 89.6° and 90.2°. We linearly interpolated the radiances of the measurements at both SZAs and then compared them to the simulation results of SZAs of 89° and 90° (see Fig. 8) to obtain the calibration factors. The simulated radiances for selected wavelengths and AODs for SZA of 89° and 90° are given in Table 3.

https://doi.org/10.5194/amt-2023-103
Preprint. Discussion started: 11 July 2023

Atmospheric Measurement Techniques Discussions

The derived calibration factors are determined for two assumptions:

a) using the simulation results for an AOD of 0.25, assuming that no information on the AOD is available (see section 2.5.2).

b) using the simulation results for the wavelength-dependent AOD derived from the simultaneous sun photometer observations (Wagner et al., 2015).

The ratios of the calibration factors for these assumptions versus the calibration factors from the original study are shown in Fig. 9. Because of the strong ozone absorption at high SZA, no reasonable calibration results with the refined method for wavelengths < 335 could be obtained. Overall slightly smaller calibration factors (between 1% and 7%) are obtained with the new method (red curve, for the case that the AOD is known) compared to the original method. This means that the calibrated spectra will have slightly higher radiances. The deviations are still within the uncertainty estimates of the original and new method (old method: ~7%, new method: about 3% to 5% between 335 and 455 nm if the AOD is known). Interestingly, for these measurements, only slightly worse calibration results are obtained if no knowledge about the exact AOD is available (blue curve). This rather good agreement is probably caused by the fact that the true AODs (between ~0.05 and 0.2, depending on wavelength, see Wagner et al., 2015) are close to the assumed AOD of 0.25).

Part of the differences might be attributed to the following reasons:

a) due to the inclusion of many non-zenith angles in the elevation sequences, the SZA range between 89° and 90° is not well covered leading to interpolation effects, because only a linear interpolation was used. These interpolation effects might cause deviations up to about 2%. In future applications, only zenith measurements should be performed for SZA>89° to better capture the SZA dependence. It should be noted that for state of the art measurements, this is already mostly implemented as standard measurement routine)

b) The uncertainties caused by the electronic offset and dark current will be higher for measurements during twilight compared to measurements at higher SZA, which determined the calibration factors of the original method. Based on a blind region of the detector we estimated the error caused by possible wrong electronic offset and dark current correction to be <1%.

Also slight deviations (1% to 3%) between the calibration factors of the new method using either the simulation results of this study (using SCIATRAN) or the simulation results of the original study (using MCARTIM) are found. Part of these deviations are caused by larger interpolation errors using the old simulation results, because they were made in steps of 2° SZA (compared to 1° in this study). The direct comparison of the results of the results of both radiative transfer models for the considered viewing geometry and atmospheric scenario yields deviations <1%.

3.1 Comparison to independent measurements

Figure 10 presents a comparison of the calibrated radiance spectrum measured on 24 June 2009 at 6:54 at a SZA=61°(blue) and a radiance spectrum measured in zenith direction under similar atmospheric conditions (clear sky, SZA = 62°) on 2 May 2007 in Hanover, Germany. Note that the measurement in Hannover was scaled by a factor of 0.97 to account for the effect of the slightly different viewing geometries (exact zenith view, compared to 85° elevation angle of our measurement, see Wagner et al., 2015). Overall, good agreement is found. Nevertheless, although the atmospheric condition and the sun-earth distance were quite similar for both measurement, no strict quantitative conclusions can be drawn from this comparison, because the measurements were not made at the same location and time.

4 Summary and conclusions

In this study we presented an improved radiance calibration method compared to our previous study (Wagner et al., 2015). The updated method uses only a short period of measurements (during twilight), whereas in the original method a much

https://doi.org/10.5194/amt-2023-103
Preprint. Discussion started: 11 July 2023

longer period (a few hours) on a day with stable aerosol conditions was required. The updated method has two main advantages: First, because of the much shorter measurement period, the method can be used on all days with cloud-free conditions during sunrise and sunset.. Second, even without knowledge about the aerosol load, the errors of the calibration method are rather small, especially in the UV spectral range (ranging from about 4% at 340 nm to 8% at 420nm). If the AOD is known, the uncertainties are even smaller (ranging from about 2% at 340 nm to 4% at 420nm). For larger wavelengths, good accuracy is only obtained if the AOD is known (ranging from about 4% at 420 nm to 10% at 700 nm). Here it should be noted that usually the AOD in the visible spectral range is systematically smaller compared to the UV.

Another important advantage is that the new calibration method can be applied retrospectively to the large number of existing zenith-sky DOAS measurements.

One disadvantage of the method is that it is not possible to determine the AOD exactly for the time of the (twilight) measurements, because AOD observations from sun photometer measurements or the MAX-DOAS measurements are only possible for SZA smaller than about 80 to 85°. Thus the AOD measured by these methods might differ from the AOD during twilight. One possibility to minimise the related uncertainty is to carry out the radiance calibration during the twilight periods of several days. Then the errors caused by variations of the AOD might largely cancel out.

It should be also noted that the variation of the earth-sun distance should be taken into account (as was done in this and the original study, see Wagner et al., 2015). If this effect is neglected errors up to about 3.2 % can arise.

The main advantage of our method compared to radiance calibration methods in the laboratory is that the calibration can be applied directly in the field. This allows routine radiance calibrations whenever the sky is cloud-free during twilight. Also, potential changes of the instrument properties during transport from the laboratory to the field are avoided.

Author contributions

TW developed the idea and wrote the paper. JP performed the radiative transfer simulations simulations and provided valuable input.

Acknowledgements

We want to thank the organisers of the Cabauw Intercomparison Campaign of Nitrogen Dioxide measuring Instruments (CINDI) in summer 2009 (https://www.knmi.nl/kennis-en-datacentrum/project/cindi), especially Ankie Piters and Marc Kroon. We thank J. S. (Bas) Henzing and his staff for their effort in establishing and maintaining the Cabauw AERONET site used in this investigation. The radiance measurements at Hanover (Fig. 9) were copied from a publication by Seckmeyer et al. (2009). We used the Radiative Transfer model SCIATRAN version 3.8.11 developed at University of Bremen (https://www.iup.uni-bremen.de/sciatran/).

Competing interests

Some authors are members of the editorial board of the journal AMT. The peer-review process was guided by an independent editor, and the authors have also no other competing interests to declare.

https://doi.org/10.5194/amt-2023-103
Preprint. Discussion started: 11 July 2023

References

Clémer, K., Van Roozendael, M., Fayt, C., Hendrick, F., Hermans, C., Pinardi, G., Spurr, R.,Wang, P., and De Mazière, M.: Multiple wavelength retrieval of tropospheric aerosol optical properties from MAXDOAS measurements in Beijing, Atmos. Meas. Tech., 3, 863–878, https://doi.org/10.5194/amt-3-863-2010, 2010.

Deutschmann, T., S. Beirle, U. Frieß, M. Grzegorski, C. Kern, L. Kritten, U. Platt, J. Pukite, T. Wagner, B. Werner, K. Pfeilsticker, The Monte Carlo Atmospheric Radiative Transfer Model McArtim: Introduction and Validation of Jacobians and 3D Features, J. Quant. Spectr. Rad. Transf., doi:10.1016/j.jqsrt.2010.12.009, 2011.

Frieß, F., Monks, P. S., Remedios, J. J., Rozanov, A., Sinreich, R., Wagner, T., and Platt, U.: MAX-DOAS O4 measurements: A new technique to derive information on atmospheric aerosols. (II) Modelling studies, J. Geophys. Res., 111, D14203, https://doi.org/10.1029/2005JD006618, 2006.

Holben, B. N., et al., AERONET—A federated instrument network and data archive for aerosol characterization, Remote Sens. Environ., 66(1), 1 – 16, 1998.

Hönninger, G., von Friedeburg, C., and Platt, U.: Multi axis differential optical absorption spectroscopy (MAX-DOAS), Atmos. Chem. Phys., 4, 231–254, https://doi.org/10.5194/acp-4- 231-2004, 2004.

Irie, H., Kanaya, Y., Akimoto, H., Iwabuchi, H., Shimizu, A., and Aoki, K.: First retrieval of tropospheric aerosol profiles using MAX-DOAS and comparison with lidar and sky radiometer measurements, Atmos. Chem. Phys., 8, 341–350, https://doi.org/10.5194/acp-8-341-2008, 2008.

Kaufman, Y. J., A. Gitelson, A. Karnieli, E. Ganor, R. S. Fraser, T. Nakajima, S. Mattoo, and B. N. Holben, Size distribution and scattering phase function of aerosol particles retrieved from sky brightness measurements, J. Geophys. Res., 99, 10,341–10,356, 1994.

Mei, L., Rozanov, V., Rozanov, A., and Burrows, J. P.: SCIATRAN software package (V4.6): update and further development of aerosol, clouds, surface reflectance databases and models, Geosci. Model Dev., 16, 1511–1536, https://doi.org/10.5194/gmd-16-1511-2023, 2023.

Niedzwiedz, A., J. Duffert, M. Tobar-Foster, E. Quadflieg, and G. Seckmeyer, Laboratory calibration for multidirectional spectroradiometers, Measurement Science and Technology, vol. 32, 2021.

Pissulla, D., Seckmeyer, G., Cordero, R. R., Blumthaler, M., Schallhart, B., Webb, A., Kift, R., Smedley, A., Bais, A. F., Kouremeti, N., Cede, A., Hermang, J., and Kowalewskig, M., Comparison of atmospheric spectral radiance measurements from five independently calibrated systems, Photochem. Photobio., 8, 516–527, 2009.

Piters, A. J. M., Boersma, K. F., Kroon, M., Hains, J. C., Van Roozendael, M., Wittrock, F., Abuhassan, N., Adams, C., Akrami, M., Allaart, M. A. F., Apituley, A., Beirle, S., Bergwerff, J. B., Berkhout, A. J. C., Brunner, D., Cede, A., Chong, J., Clémer, K., Fayt, C., Frieß, U., Gast, L. F. L., Gil-Ojeda, M., Goutail, F., Graves, R., Griesfeller, A., Großmann, K., Hemerijckx, G., Hendrick, F., Henzing, B., Herman, J., Hermans, C., Hoexum, M., van der Hoff, G. R., Irie, H., Johnston, P. V., Kanaya, Y., Kim, Y. J., Klein Baltink, H., Kreher, K., de Leeuw, G., Leigh, R., Merlaud, A., Moerman, M. M., Monks, P. S., Mount, G. H., Navarro-Comas, M., Oetjen, H., Pazmino, A., Perez-Camacho, M., Peters, E., du Piesanie, A., Pinardi, G., Puentedura, O., Richter, A., Roscoe, H. K., Schönhardt, A., Schwarzenbach, B., Shaiganfar, R., Sluis, W., Spinei, E., Stolk, A. P., Strong, K., Swart, D. P. J., Takashima, H., Vlemmix, T., Vrekoussis, M., Wagner, T., Whyte, C., Wilson, K. M., Yela, M., Yilmaz, S., Zieger, P., and Zhou, Y.: The Cabauw Intercomparison campaign for Nitrogen Dioxide measuring Instruments (CINDI): design, execution, and early results, Atmos. Meas. Tech., 5, 457–485, doi:10.5194/amt-5-457-2012, 2012.

Riechelmann, S., M. Schrempf, and G. Seckmeyer, Simultaneous measurement of spectral sky radiance by a non-scanning multidirectional spectroradiometer (MUNDIS) Meas. Sci. Technol. 24 8, 2013.

https://doi.org/10.5194/amt-2023-103
Preprint. Discussion started: 11 July 2023

Atmospheric Measurement Techniques Discussions

Rozanov, V. V., Dinter, T., Rozanov, A. V., Wolanin, A., Bracher, A., and Burrows, J. P.: Radiative transfer modeling through terrestrial atmosphere and ocean accounting for inelastic processes: Software package SCIATRAN, J. Quant. Spectrosc. Ra., 194, 65–85, 2017.

Tanre, D., C. Deuaux, M. Herman, and R. Santer, Radiative properties of desert aerosols by optical ground-based measurements at solar wavelengths, J. Geophys. Res., 93, 14,223– 14,231, 1988.

Volz, F. E., Photometer mit Selen-Photoelement zur spektralen Messung der Sonnenstrahlung und zur Bestimmung der Wellenlangenabhängigkeit der Dunsttrübung, Arch. Meteorol. Geophys. Bioklimatol., Ser. B, l0, 100– 131, 1959.

Wagner, T., Dix, B., von Friedeburg, C., Frieß, U., Sanghavi, S., Sinreich, R., and Platt, U.: MAX-DOAS O4 measurements – a new technique to derive information on atmospheric aerosols. (I) Principles and information content, J. Geophys. Res., 109, D22205, https://doi.org/10.1029/2004JD004904, 2004

Wagner, T., Beirle, S., Dörner, S., Penning de Vries, M., Remmers, J., Rozanov, A., and Shaiganfar, R.: A new method for the absolute radiance calibration for UV–vis measurements of scattered sunlight, Atmos. Meas. Tech., 8, 4265–4280, https://doi.org/10.5194/amt-8-4265-2015, 2015.

Wagner, T., Dörner, S., Beirle, S., Donner, S., and Kinne, S.: Quantitative comparison of measured and simulated O_4 absorptions for one day with extremely low aerosol load over the tropical Atlantic, Atmos. Meas. Tech., 14, 3871–3893, https://doi.org/10.5194/amt-14-3871-2021, 2021.

Wuttke S, Seckmeyer G, Bernhard G, Ehramjian J, McKenzie R, Johnston P and O'Neill M., New spectroradiometers complying with the NDSC standards J. Atmos. Ocean. Technol., 23, 241–251, 2006.

Yu X, Sun Y, Fang A, Qi W and Liu C., Laboratory spectral calibration and radiometric calibration of hyper-spectral imaging spectrometer The 2014 2nd Int. Conf. on Systems and Informatics (ICSAI 2014) pp 871–5, 2014.

Tables

Table 1 Settings used for the radiative transfer simulations

Parameter	Standard scenario	Variations
polarisation	yes	no
temperature profile	US standard atmosphere	+20 K
pressure profile	US standard atmosphere	-2 %
O_3 profile	US standard atmosphere	+20 %
surface albedo	0.05	0.03, 0.07
Surface altitude	0 m	1000 m
elevation angle	90°	88° (rel. Azimuth angle: 0, 90°)
Raman scattering*	no	yes
AOD	0.1, 0.3	0, 0.02, 0.05, 0.1, 0.2, 0.3, 0.5, 1
aerosol layer height	1000 m	200m, 500m, 2000m
single scattering albedo	0.95	0.9, 1.0
phase function	urban	Marine, biomass burning
stratospheric aerosols**	yes	no

*For the investigation of the effect of Raman scattering the simulated spectra are convoluted with a FWHM of 0.6nm and then the average of the radiance for +/-0.25 nm around the selected wavelength is taken

**AOD of 0.012 between 18 and 33km, see Wagner et al. (2021)

https://doi.org/10.5194/amt-2023-103
Preprint. Discussion started: 11 July 2023

Atmospheric Measurement Techniques Discussions

335

Table 2 Assumptions made for the quantification of different sources of uncertainty

Quantity	**Tested variation**	**Weighting of the simulation results to obtain the radiance error displayed in Figs. 6 and 7**
Ozone	original ozone profile or profile increased by 20%	difference between both simulations
Temperature	original temperature profile or profile increased by 20K	half difference between both simulations
Pressure	original pressure profile or profile decreased by 2%	half difference between both simulations
Surface albedo	surface albedo 0.03 or 0.07	half difference between both simulations
Aerosol layer height	layer height 200m or 2000m	half difference between both simulations
Aerosol phase function	biomass burning and marine aerosols	half difference between both simulations
Aerosol single scattering albedo (SSA)	SSA of 0.9 and SSA of 1.0	half difference between both simulations
Stratospheric aerosols	scenarios with or without stratospheric aerosols	half difference between both simulations
Polarisation	simulations with or without polarisation	difference between both simulations
Raman scattering	simulations with or without Raman scattering	difference between both simulations
Instrument elevation	simulations at sea level or 1 km altitude	10% of the difference between both simulations
Pointing accuracy in the plane towards the sun	elevation angles of 88° and 90°	difference between both simulations
Pointing accuracy perpendicular to the plane towards the sun	elevation angles of 88° and 90°	difference between both simulations

340

345

350

355

https://doi.org/10.5194/amt-2023-103
Preprint. Discussion started: 11 July 2023

Atmospheric Measurement Techniques Discussions

360

Table 3 Zenith scattered normalised radiances at SZA of 89° and 90° for different wavelenghts, AODs and for the standard settings (see table 1).

	SZA = 89°							SZA = 90°					
Wavelength [nm]	AOD = 0.1	AOD = 0.2	AOD = 0.3	AOD = 0.5	AOD = 0.7	AOD = 1		AOD = 0.1	AOD = 0.2	AOD = 0.3	AOD = 0.5	AOD = 0.7	AOD = 1
340	0.00236	0.00239	0.00242	0.00246	0.00249	0.00249		0.00152	0.00154	0.00156	0.00158	0.00160	0.00160
350	0.00261	0.00266	0.00270	0.00275	0.00279	0.00281		0.00171	0.00174	0.00176	0.00180	0.00182	0.00183
360	0.00263	0.00268	0.00273	0.00279	0.00284	0.00286		0.00172	0.00175	0.00178	0.00183	0.00186	0.00187
370	0.00265	0.00270	0.00275	0.00283	0.00288	0.00292		0.00173	0.00177	0.00181	0.00186	0.00189	0.00192
380	0.00265	0.00271	0.00277	0.00285	0.00291	0.00296		0.00174	0.00178	0.00182	0.00188	0.00191	0.00194
390	0.00265	0.00272	0.00278	0.00287	0.00294	0.00299		0.00174	0.00179	0.00183	0.00189	0.00193	0.00197
400	0.00264	0.00272	0.00278	0.00289	0.00296	0.00302		0.00174	0.00179	0.00184	0.00190	0.00195	0.00199
410	0.00264	0.00272	0.00279	0.00290	0.00297	0.00304		0.00174	0.00179	0.00184	0.00191	0.00197	0.00201
420	0.00263	0.00272	0.00279	0.00291	0.00299	0.00307		0.00174	0.00180	0.00185	0.00192	0.00198	0.00203
430	0.00262	0.00271	0.00278	0.00291	0.00300	0.00308		0.00174	0.00180	0.00185	0.00193	0.00199	0.00205
440	0.00259	0.00268	0.00276	0.00289	0.00298	0.00307		0.00172	0.00178	0.00183	0.00192	0.00198	0.00204
450	0.00256	0.00266	0.00274	0.00287	0.00297	0.00306		0.00171	0.00177	0.00182	0.00191	0.00198	0.00204
460	0.00250	0.00259	0.00267	0.00281	0.00291	0.00300		0.00166	0.00172	0.00178	0.00187	0.00194	0.00200
470	0.00247	0.00257	0.00265	0.00279	0.00289	0.00299		0.00165	0.00172	0.00178	0.00187	0.00194	0.00201
480	0.00235	0.00244	0.00253	0.00266	0.00276	0.00286		0.00157	0.00163	0.00169	0.00178	0.00185	0.00192
490	0.00232	0.00242	0.00250	0.00264	0.00274	0.00285		0.00155	0.00162	0.00168	0.00177	0.00184	0.00191
500	0.00219	0.00228	0.00236	0.00250	0.00260	0.00270		0.00146	0.00152	0.00158	0.00167	0.00174	0.00181
510	0.00207	0.00216	0.00224	0.00238	0.00248	0.00258		0.00138	0.00145	0.00150	0.00159	0.00166	0.00172
520	0.00198	0.00207	0.00215	0.00228	0.00237	0.00247		0.00132	0.00138	0.00144	0.00152	0.00159	0.00166
530	0.00175	0.00183	0.00190	0.00202	0.00211	0.00220		0.00116	0.00121	0.00126	0.00134	0.00140	0.00146
540	0.00168	0.00175	0.00182	0.00194	0.00203	0.00212		0.00111	0.00116	0.00121	0.00129	0.00134	0.00140
550	0.00156	0.00163	0.00170	0.00181	0.00190	0.00198		0.00103	0.00108	0.00113	0.00120	0.00125	0.00131
560	0.00142	0.00149	0.00155	0.00166	0.00174	0.00182		0.00094	0.00098	0.00102	0.00109	0.00114	0.00119
570	0.00127	0.00134	0.00139	0.00149	0.00156	0.00164		0.00083	0.00087	0.00091	0.00097	0.00102	0.00106
580	0.00126	0.00132	0.00138	0.00147	0.00155	0.00163		0.00083	0.00087	0.00091	0.00097	0.00101	0.00106
590	0.00126	0.00133	0.00138	0.00148	0.00156	0.00164		0.00084	0.00088	0.00092	0.00098	0.00103	0.00108
600	0.00113	0.00119	0.00124	0.00133	0.00140	0.00148		0.00074	0.00078	0.00082	0.00087	0.00092	0.00096
610	0.00116	0.00122	0.00128	0.00138	0.00145	0.00153		0.00078	0.00082	0.00085	0.00091	0.00096	0.00101
620	0.00124	0.00131	0.00137	0.00148	0.00157	0.00165		0.00085	0.00089	0.00093	0.00100	0.00105	0.00111
630	0.00129	0.00137	0.00143	0.00155	0.00164	0.00173		0.00090	0.00094	0.00099	0.00106	0.00111	0.00117
640	0.00136	0.00144	0.00151	0.00163	0.00173	0.00183		0.00096	0.00101	0.00106	0.00113	0.00119	0.00125
650	0.00141	0.00149	0.00157	0.00170	0.00181	0.00192		0.00101	0.00106	0.00111	0.00120	0.00126	0.00133
660	0.00145	0.00154	0.00162	0.00176	0.00187	0.00198		0.00105	0.00110	0.00116	0.00124	0.00131	0.00138
670	0.00149	0.00158	0.00166	0.00181	0.00192	0.00205		0.00108	0.00115	0.00120	0.00129	0.00136	0.00144
680	0.00151	0.00161	0.00170	0.00185	0.00197	0.00210		0.00111	0.00118	0.00123	0.00133	0.00140	0.00148
690	0.00152	0.00162	0.00171	0.00187	0.00199	0.00213		0.00113	0.00119	0.00125	0.00135	0.00142	0.00150
700	0.00153	0.00164	0.00173	0.00189	0.00202	0.00216		0.00114	0.00121	0.00127	0.00137	0.00145	0.00153

365

370

375

380

https://doi.org/10.5194/amt-2023-103
Preprint. Discussion started: 11 July 2023

Atmospheric Measurement Techniques Discussions

Figures

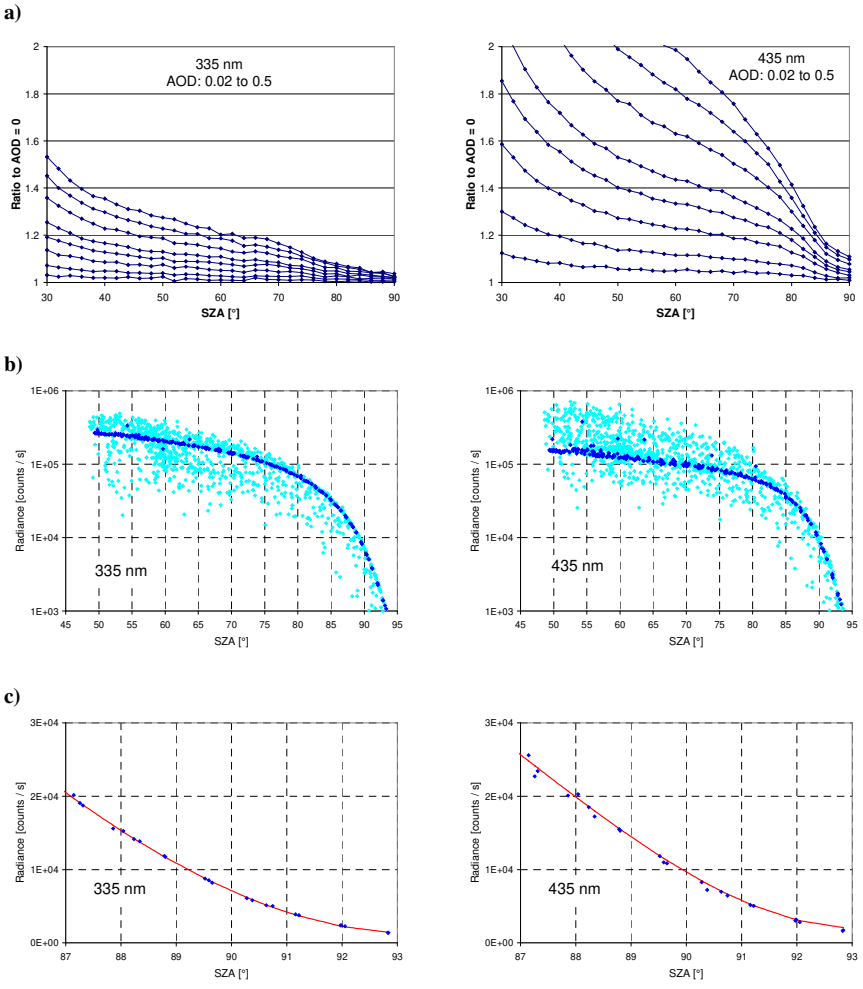

385 **Fig. 1 a) Ratio of the simulated zenith radiance for different aerosol optical depths to the radiance for an atmosphere without aerosols as function of the SZA for 335 nm (left) and 435 nm (right). Data are taken from Fig. 5 in Wagner et al. (2015). In that study simulations were only performed for SZA up to 90°. AOD values are 0.02, 0.05, 0.1, 0.15, 0.2, 0.3, 0.4, 0.5. At 90° SZA, the variation of the radiance is smallest (about 4 % at 335 nm and 11 % at 435 nm). b) measured zenith radiances from 19 Septenber to 18 October 2022 in Mainz, Germany, for all sky conditions (light**
390 **blue) and clear sky conditions (dark blue). c) radiances during cloud-free conditions together with a fitted polynomial (for SZA between 85° and 93°).**

395

https://doi.org/10.5194/amt-2023-103
Preprint. Discussion started: 11 July 2023

Atmospheric Measurement Techniques Discussions

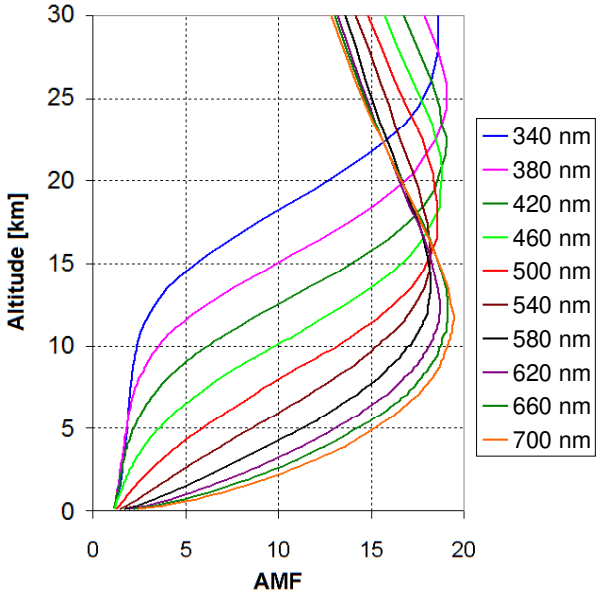

Fig. 2 Altitude dependence of the box-AMFs for observations of zenith-scattered sun light during twilight (averages for simulations at SZA of 89° and 90°). Box-AMFs close to unity indicate an almost vertical light path. Simulations are performed for an atmosphere without aerosols.

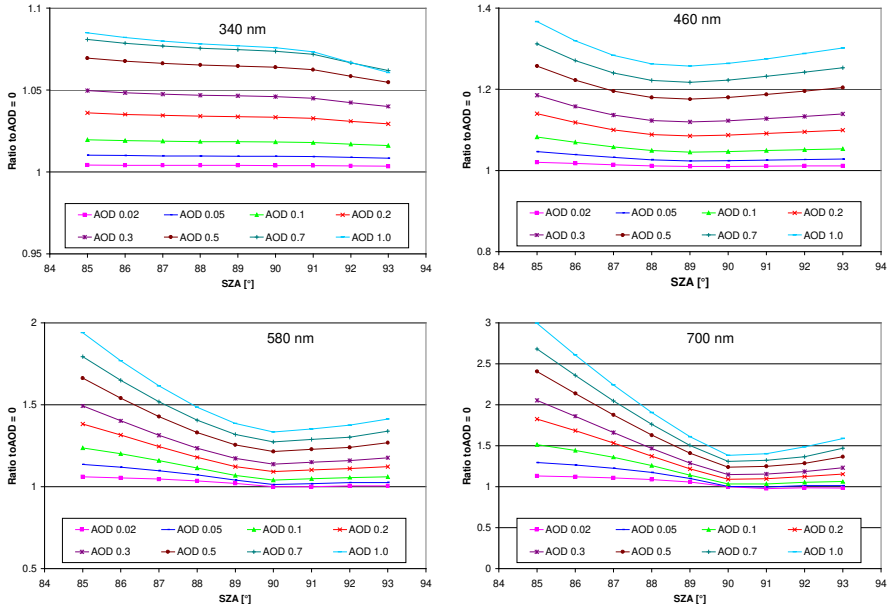

Fig. 3 Ratio of the simulated radiances for different AODs compared to the simulation results without aerosols as function of the SZA for the standard scenario, see Table 1. Results for additional wavelengths are shown in Fig. A1 in the appendix. Note the different y-axes.

https://doi.org/10.5194/amt-2023-103
Preprint. Discussion started: 11 July 2023

Atmospheric Measurement Techniques Discussions

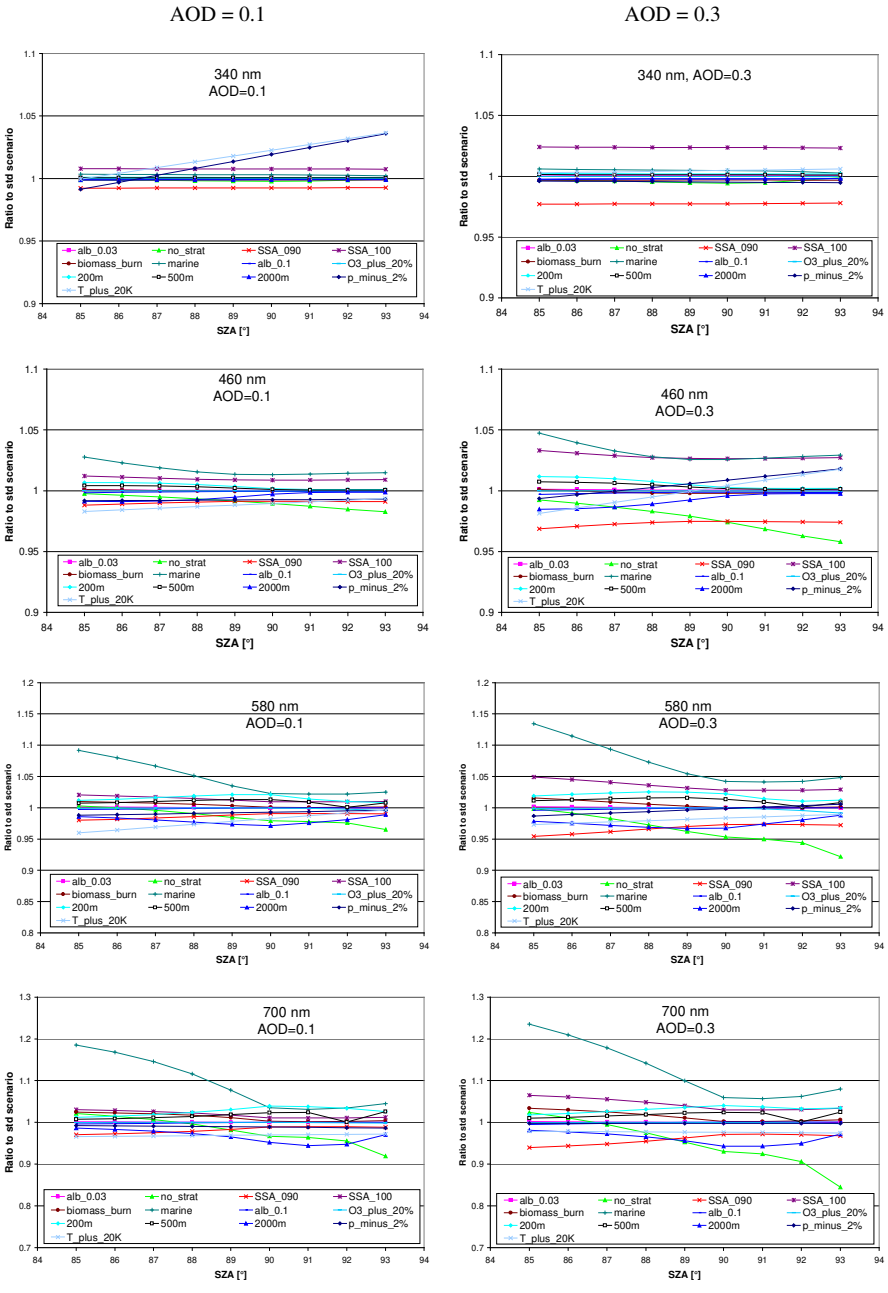

Fig. 4 Ratio of the simulated radiance for different aerosol properties and further input parameters compared to the radiances for the corresponding standard scenarios for AOD of 0.1 (left) and 0.3 (right) as function of the SZA. Note the different y-axes. Results for additional wavelengths are shown in Fig. A2 in the appendix.

https://doi.org/10.5194/amt-2023-103
Preprint. Discussion started: 11 July 2023

Atmospheric Measurement Techniques Discussions

415

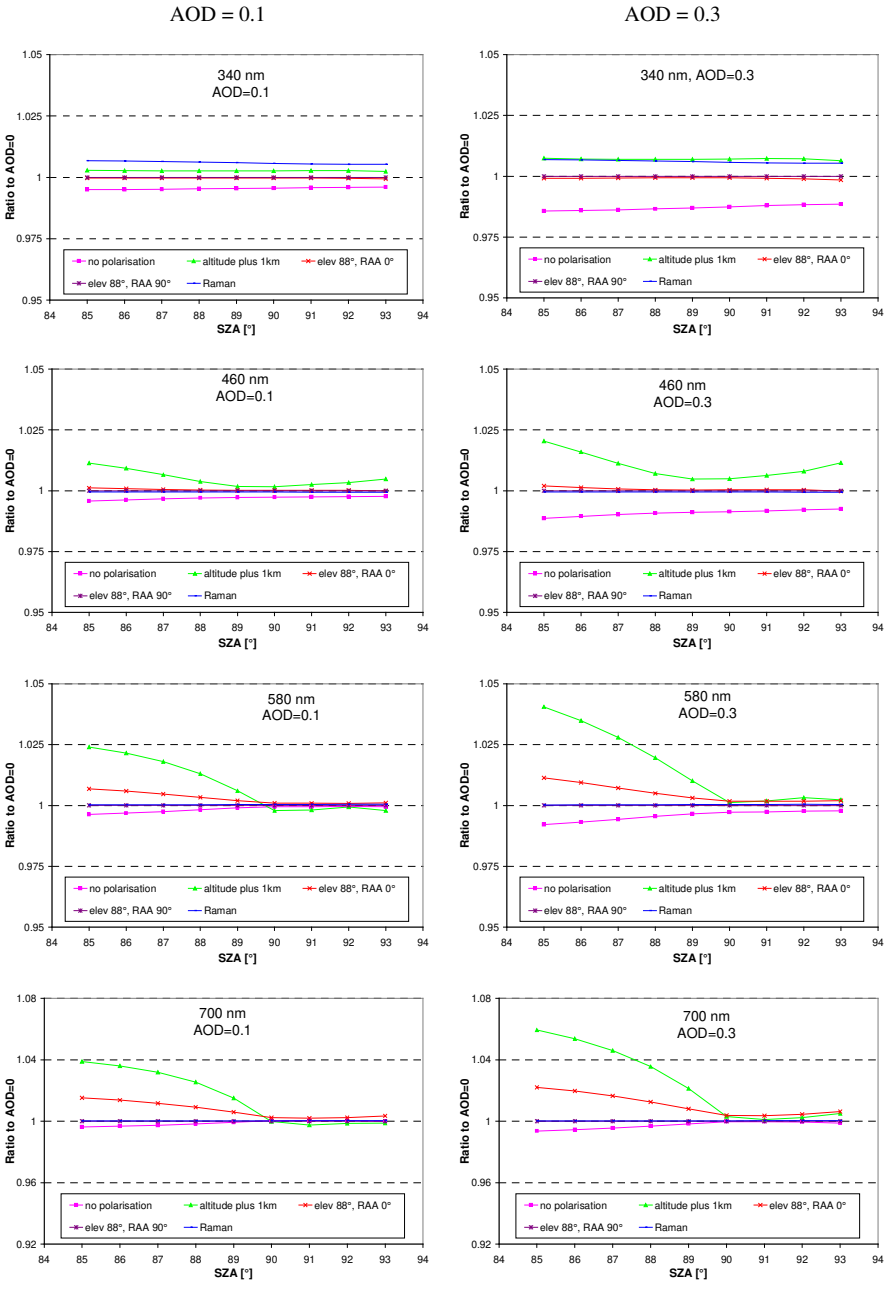

Fig. 5 Ratio of the simulated radiances for different instrumental properties and chosen options of the radiative transfer simulations compared to the radiances of the corresponding standard scenarios for AOD of 0.1 (left) and 0.3 (right) as function of the SZA. Note the different y-axes. Results for additional wavelengths are shown in Fig. A3 in the appendix.

420

https://doi.org/10.5194/amt-2023-103
Preprint. Discussion started: 11 July 2023

Atmospheric Measurement Techniques Discussions

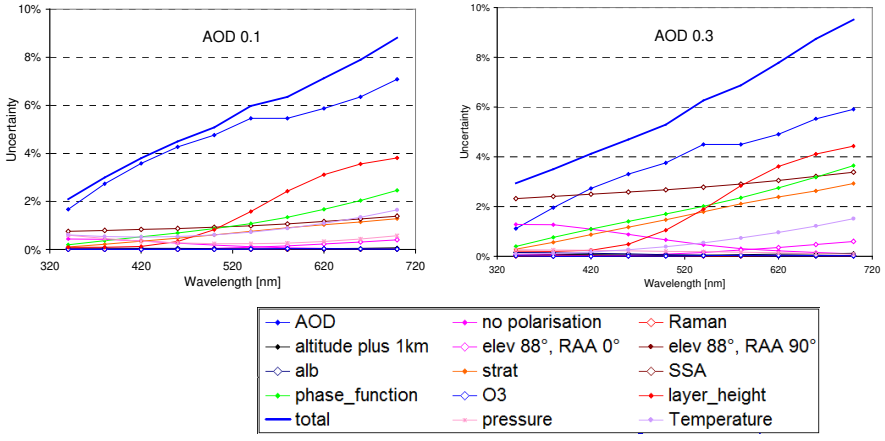

Fig. 6 Total and individual errors for the scenario with AOD of 0.1 (left) and 0.3 (right) for zenith measurements during twilight (SZA between 89° and 90°).

425

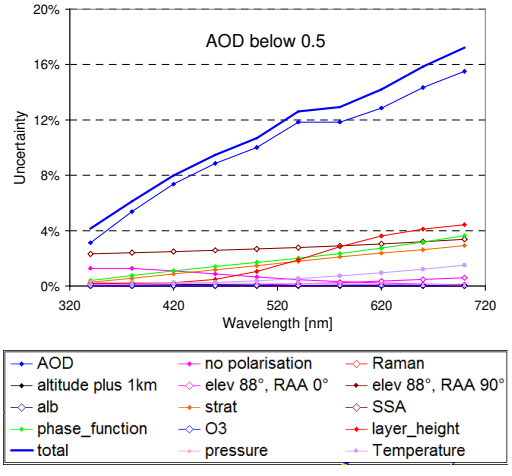

430 **Fig. 7 Total and individual errors for the scenario with AOD of 0.25 ±0.125 for zenith measurements during twilight (SZA between 89° and 90°).**

435

440

https://doi.org/10.5194/amt-2023-103
Preprint. Discussion started: 11 July 2023

Atmospheric Measurement Techniques Discussions

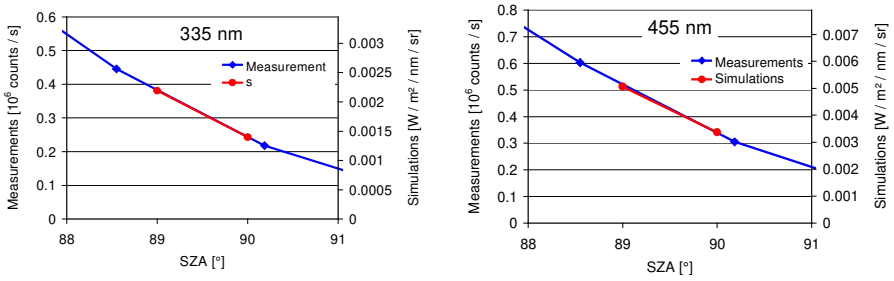

Fig. 8 Examples of the determination of the calibration factors for two selected wavelengths. The linearly interpolated measurement results (blue) are compared to the linearly interpolated simulation results for the standard scenario (red).

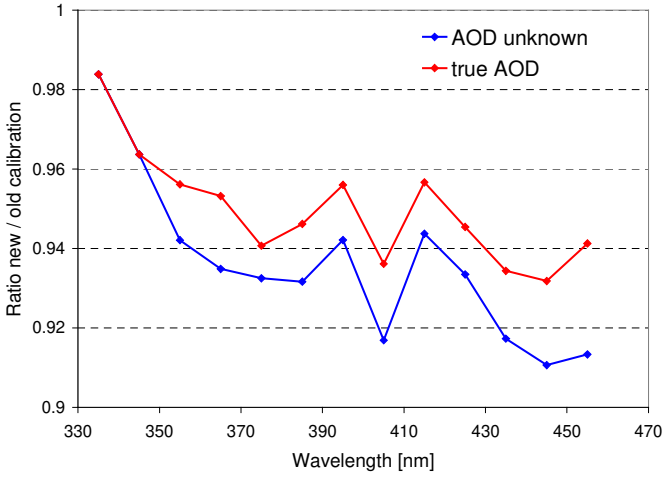

Fig. 9 Ratio of the calibration factors for the scenarios with unknown AOD (blue) and known AOD (red) versus the calibration factors of the original study (values <1 mean that the new calibration leads to higher radiances).

https://doi.org/10.5194/amt-2023-103
Preprint. Discussion started: 11 July 2023

Atmospheric Measurement Techniques Discussions

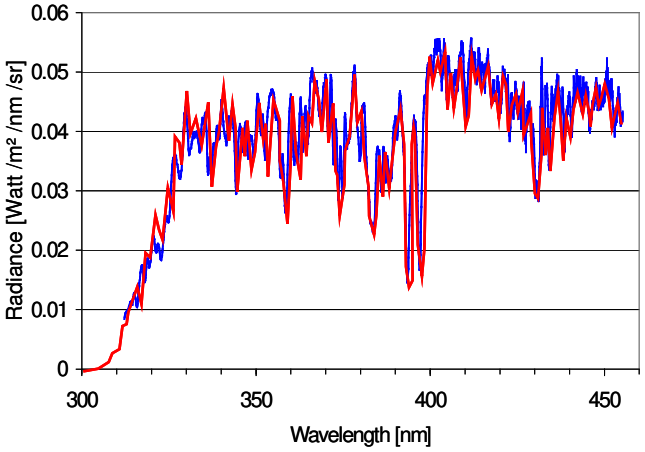

Fig. 10 Comparison of a calibrated spectrum (blue), measured on 24 June 2009, 6:54, at a SZA of 61° to an independent measurement under similar conditions (red) on 2 May, 2007 in Hannover, Germany (clear sky, SZA: 62°, Seckmeyer et al., 2009). The measurement in Hannover was scaled by a factor of 0.97 to account for the effect of the slightly different viewing geometries: The measurements in Hannover were made at exact zenith view, while our measurements were made at 85° elevation. (the figure is similar to Fig. 9 in Wagner et al., 2015)

Appendix

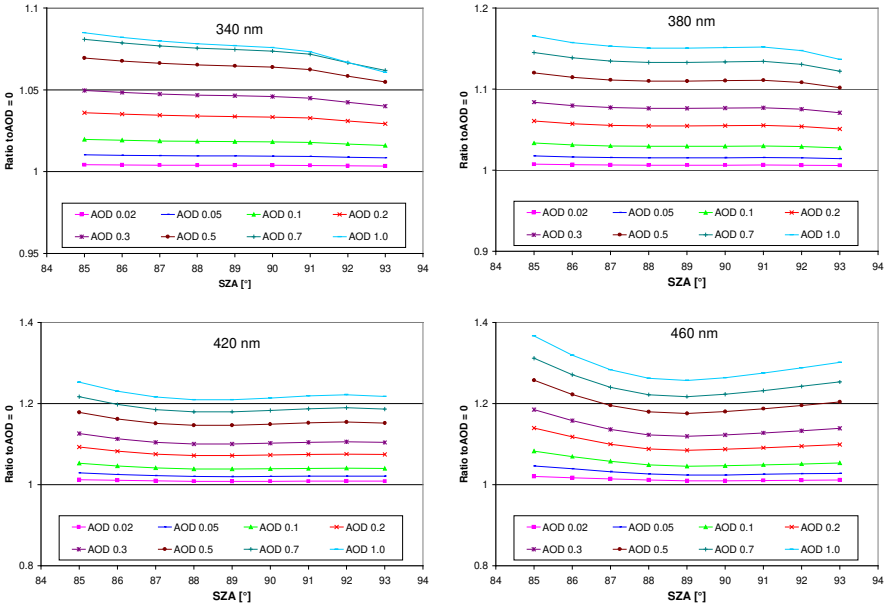

https://doi.org/10.5194/amt-2023-103
Preprint. Discussion started: 11 July 2023

Atmospheric Measurement Techniques Discussions

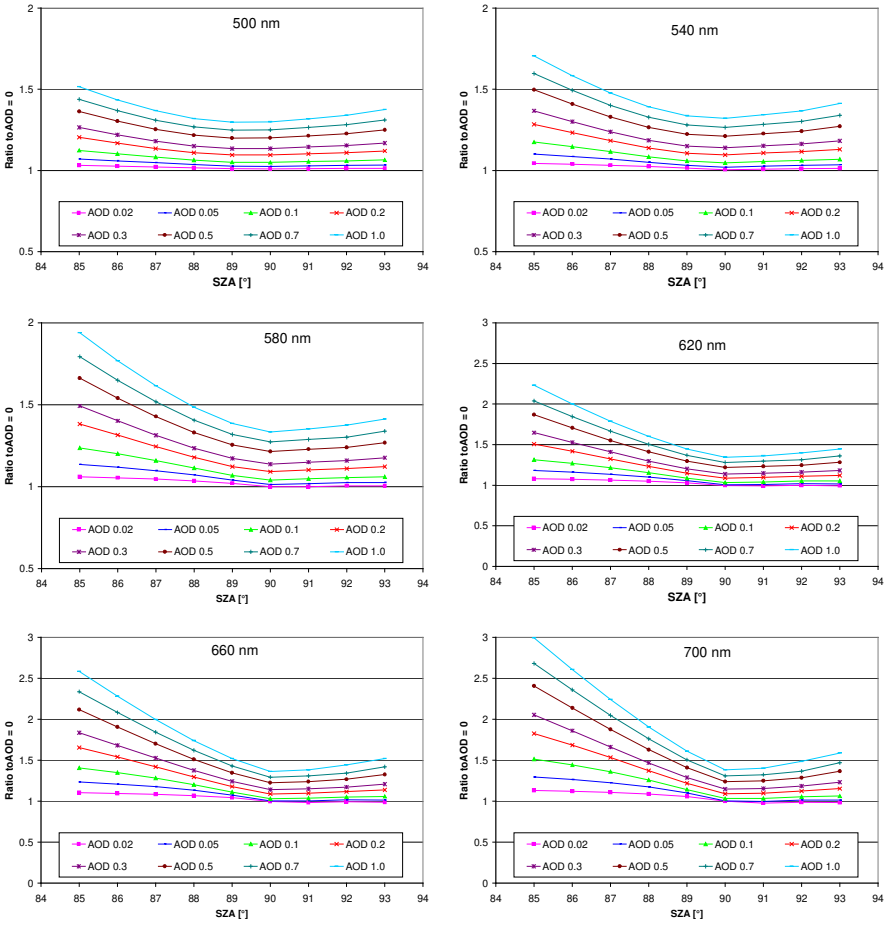

Fig. A1 Ratio of the simulated radiances for different AODs compared to the simulation results without aerosols as function of the SZA for the standard scenario, see Table 1. Note the different y-axes.

465

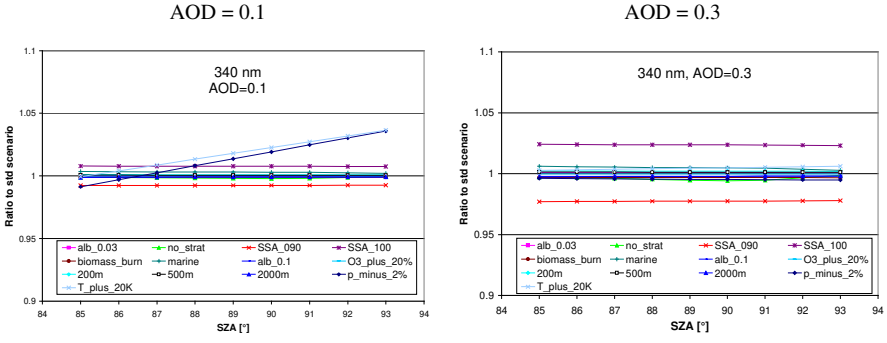

https://doi.org/10.5194/amt-2023-103
Preprint. Discussion started: 11 July 2023

Atmospheric Measurement Techniques Discussions

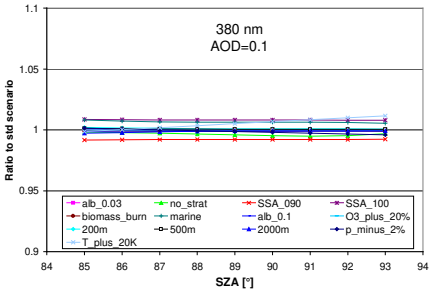

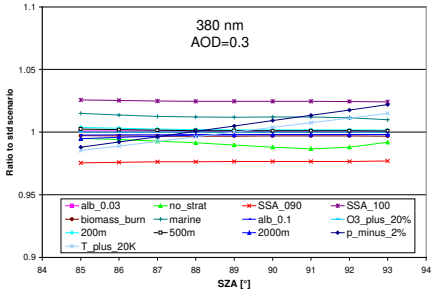

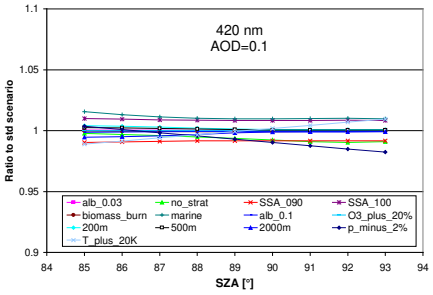

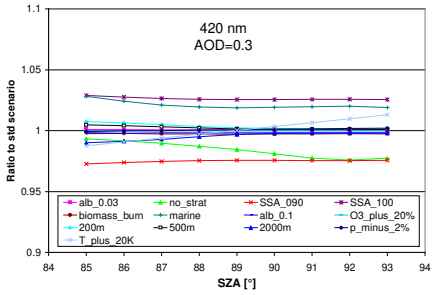

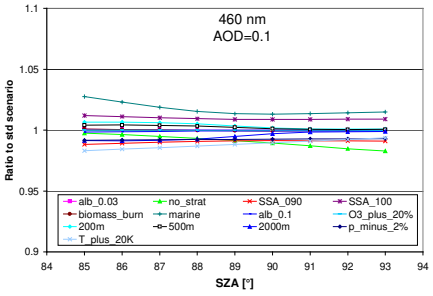

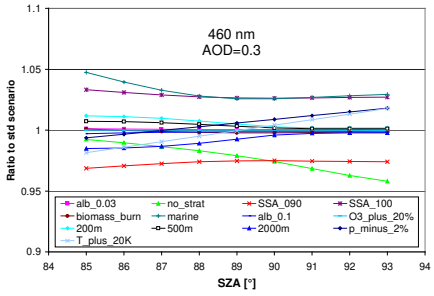

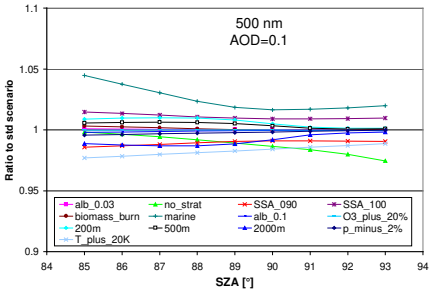

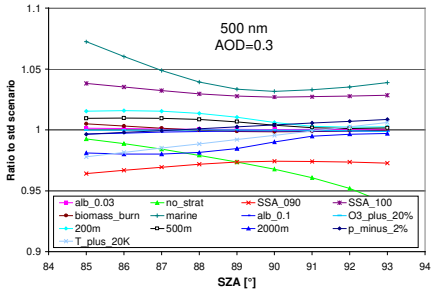

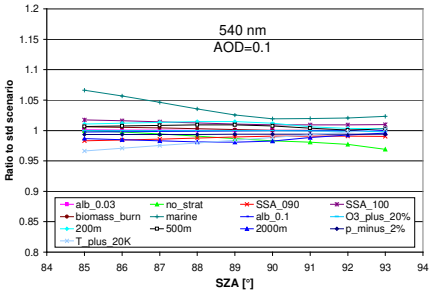

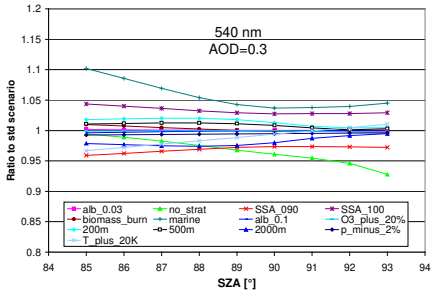

https://doi.org/10.5194/amt-2023-103
Preprint. Discussion started: 11 July 2023

Atmospheric Measurement Techniques Discussions

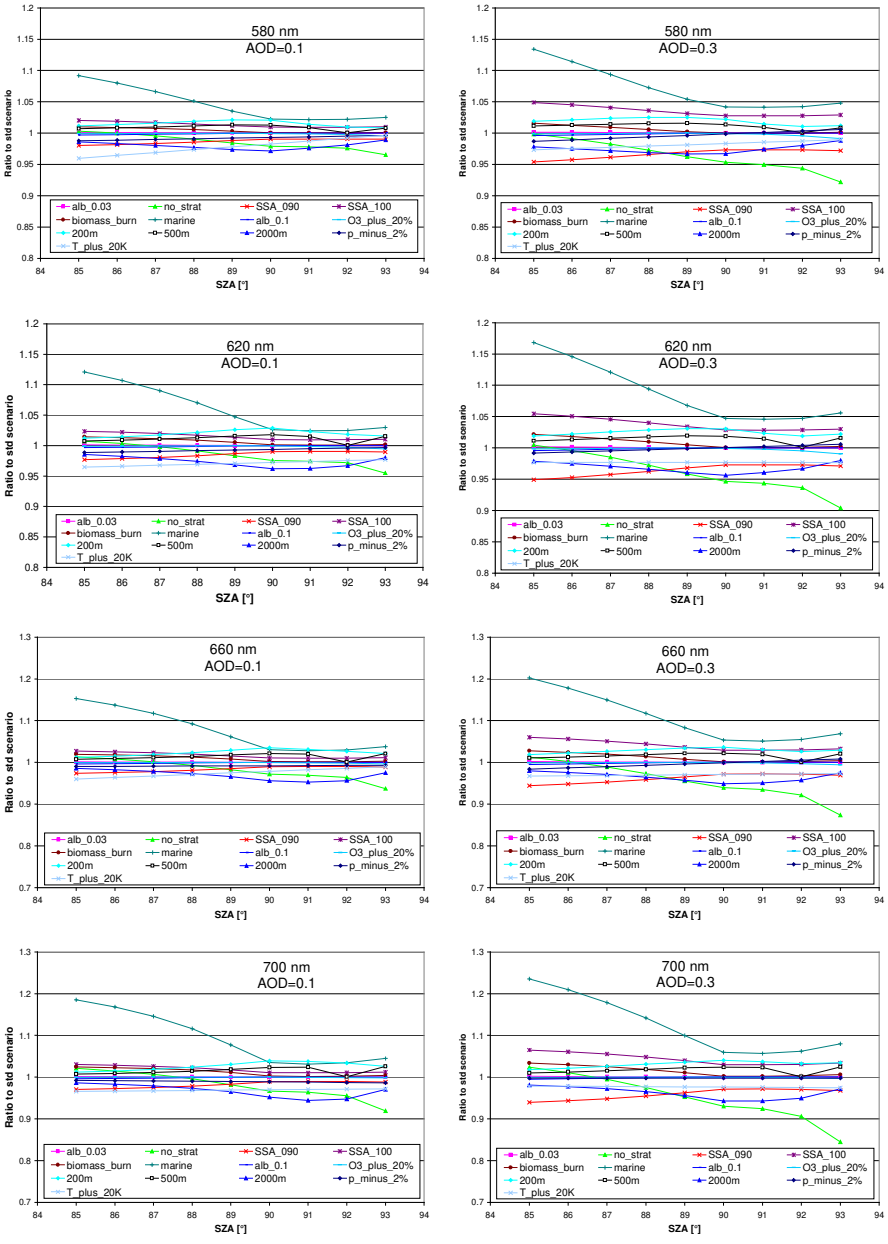

Fig. A2 Ratio of the simulated radiance for different aerosol properties and further input parameters compared to the radiances for the corresponding standard scenarios for AOD of 0.1 (left) and 0.3 (right) as function of the SZA. Note the different y-axes.

https://doi.org/10.5194/amt-2023-103
Preprint. Discussion started: 11 July 2023

Atmospheric Measurement Techniques Discussions

AOD = 0.1 AOD = 0.3

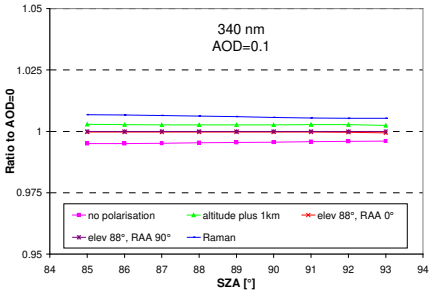

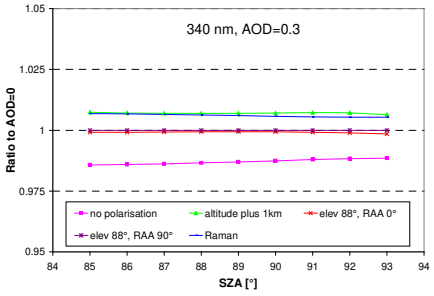

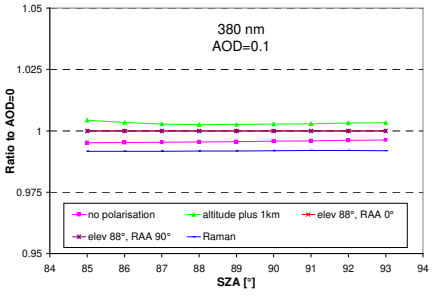

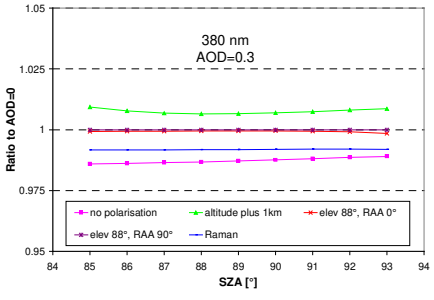

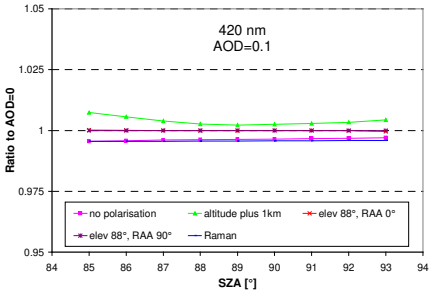

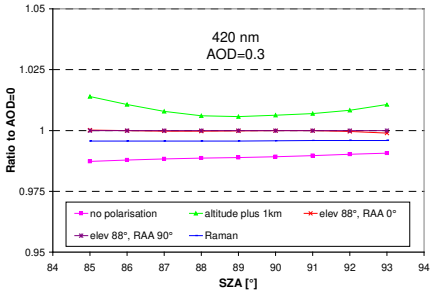

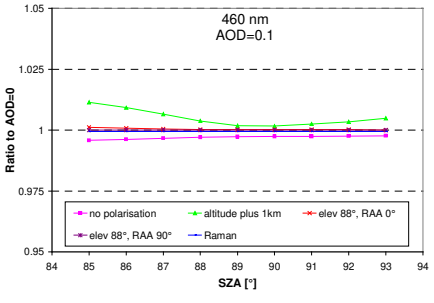

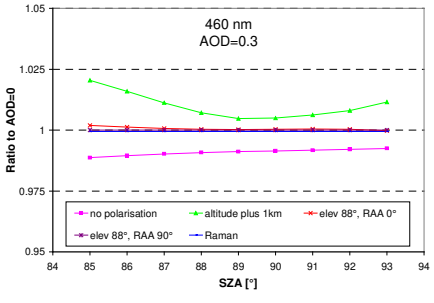

https://doi.org/10.5194/amt-2023-103
Preprint. Discussion started: 11 July 2023

Atmospheric Measurement Techniques Discussions

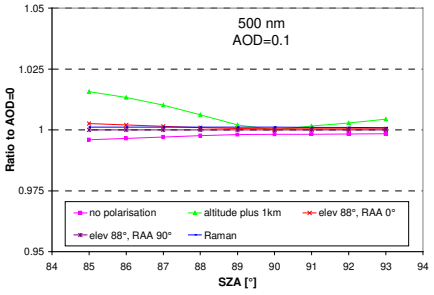

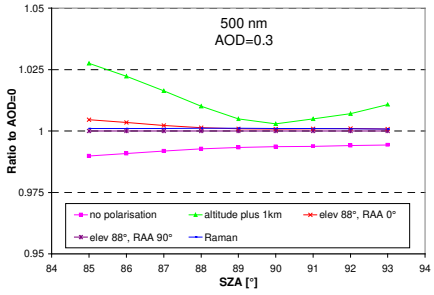

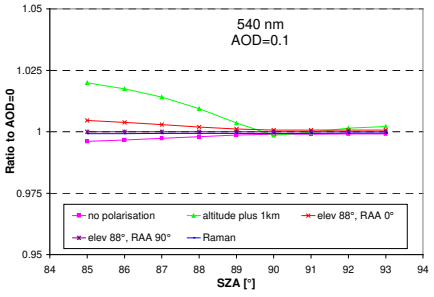

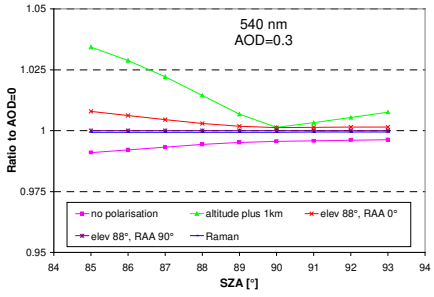

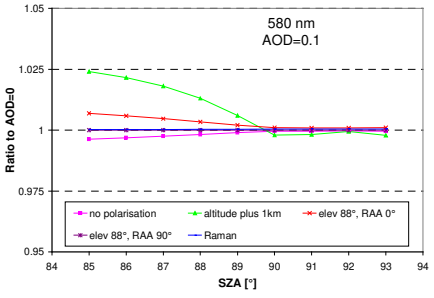

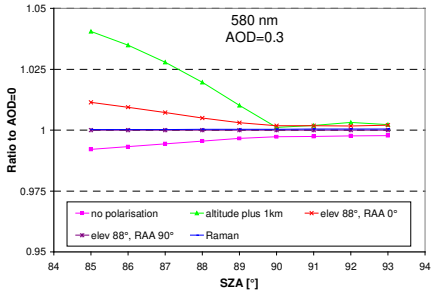

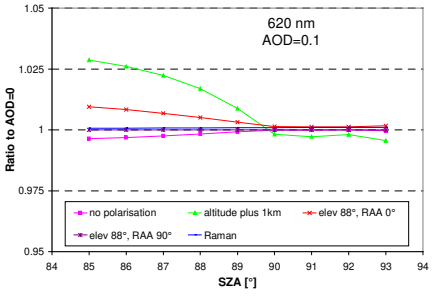

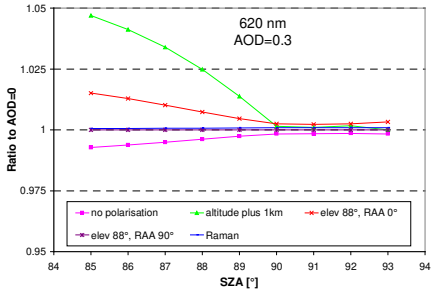

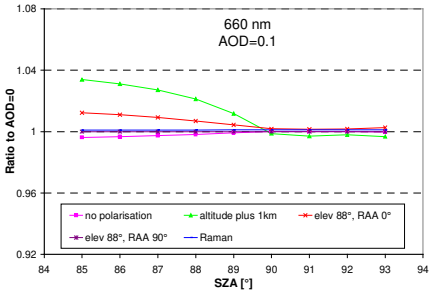

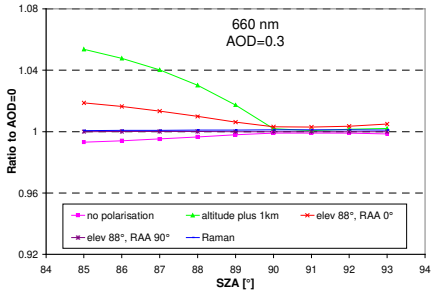

https://doi.org/10.5194/amt-2023-103
Preprint. Discussion started: 11 July 2023

Atmospheric Measurement Techniques Discussions

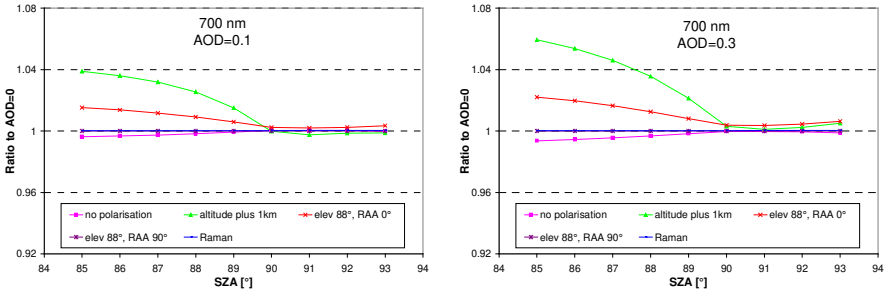

Fig. A3 Ratio of the simulated radiances for different instrumental properties and chosen options of the radiative transfer simulations compared to the radiances of the corresponding standard scenarios for AOD of 0.1 (left) and 0.3 (right) as function of the SZA.Note the different y-axes.

480